

Comparison of nano-hydroxyapatite productivity by *Pseudomonas aeruginosa* and *Serratia marcescens* through encapsulation method

Anita Khanafari^{1*}, Tayebeh Akbari¹, Mahmoud Reza Sohrabi²

¹Microbiology Department, North Tehran Branch, Islamic Azad University, Tehran, Iran

²Chemistry Department, North Tehran Branch, Islamic Azad University, Tehran, Iran

Abstract

Objective(s): The production of nano-hydroxyapatite by two encapsulated bacterial strains was the goal of current research.

Materials and Methods: *Serratia marcescens* ATCC 14756 and *Pseudomonas aeruginosa* PTCC 1570 were used by two methods including encapsulated form in 2% (w/v) alginate sodium powder and inoculated form (10%) in nutrient broth medium containing alginate sodium blank beads. In both cases alginate beads transferred to calcium and phosphorus precursors mineral medium for 48 h and were incubated at 32-35 °C for 14 days. To obtain hydroxyapatite powder, alginate beads were dried at 60 °C and rubbed. Sol-gel as chemical method was used for comparing with microbial analysis. The nature of produced powders was evaluated in each step by XRD, FTIR and scanning electron microscopy.

Results: The results showed that the yield rate of sol-gel method was 18.3% and it was much more than encapsulated method (3.032 and 3.203 w/w dried alginate bead). The size of the particles in microbial method were smaller (8-68 nm cylindrical particles and 12-55 and 15-37 nm spherical particles) than chemical method (350-880 nm of cylindrical and 34-67 nm of spherical particles).

Conclusion: Nanoparticle sizes and distribution of microbial nano-hydroxyapatite powder samples shows that it has excellent physical properties similar to natural bone and may be to produce dense and porous bioactive bone implants with desired properties.

Keywords: Alginate beads, Hydroxylapatite, Nanoscale, *Pseudomonas aeruginosa*, *Serratia marcescens*

*Corresponding Author: Anita Khanafari, Microbiology Department, North Tehran Branch, Islamic Azad University, Tehran, Iran.
Tel: +9821 2295 5900, Email: khanafari_a@yahoo.com,

Introduction

Hydroxyapatite (HA) or bioceramics [$\text{Ca}_{10}(\text{PO}_4)_6(\text{OH})_2$] was first identified as being the mineral component of bone in 1926 by DeJong (1, 2). But now due to its similarity to the main mineral of bone, extraordinary bioactivity, biocompatibility, osteo conductivity, noninflammatory, nontoxicity, nonimmunogenic nature, great thermo dynamic stability at physiological pH (1-4). It is specially developed for medical and dentistry applications such as used in bone substituent materials (5-8), constituent implants and dental materials (3), scaffolds for tissue engineering (6, 9), deliver pharmacological matters with sustained release capacity for the treatment of osteoporosis, osteomyelitis, osseous cancers and etc (2). The property of hydroxyapatite including its high bioactivity and particular adsorb ability for various ions and organic molecules has suited it for non-medical applications like packing media for chromatography column, gas sensors, catalysts and etc (6). Production of materials with nanostructures for biomaterials application has been interested in this century (3). Calcium phosphate presence in bone is in the form of nano-sized needlelike crystals of nearly 5-20 nm width and 60 nm lengths, with an inconsiderable crystallized nonstoichiometric apatite phase containing CO_3^{2-} , Na^+ , F^- and other ions in a collagen fiber matrix (8). Scale of nano is a very important parameter to enhance the contact and stability at the natural/artificial interface of bone (6, 8). Nano HA particles are similar to the apatite crystals of tooth enamel in morphology, crystal structure and crystallinity (6, 10). Moreover, studies on the in vitro and in vivo Ca^{2+} ions release from the nano HA powders were discovered to be similar to bone apatite and meaningfully faster than micro scale sized counterparts (6). Several methods have been developed for calcium phosphate synthesis, considering its multiple applications in biomedical

fields. These methods include mechanochemical synthesis (11-13), hydrothermal synthesis (14, 15), multiple emulsion technique (16), deposition technique (17, 18), precipitation (19, 20), electrodeposition technique (21), hydrolysis (22, 23), Sol-gel procedure as a preferred method over the chemical methods (24-27) and biomineralization as a new cost effective and versatile method (28, 29).

These techniques lead to generation of nano to micrometric size HA crystals (6).

The goal of current research was focused on ability of two biofilm producing bacterial strains, *Serratia marcescens* ATCC 14756 and *Pseudomonas aeruginosa* PTCC 1570, to biosynthesis hydroxyapatite (HA) in nano scale via encapsulation in alginate beads and its comparison with Sol-gel procedure as a common chemical method.

Materials and Methods

Materials

All of following chemicals were supplied by Merck, Germany.

Two standard bacterial strains, *Serratia marcescens* ATCC 14756 and *Pseudomonas aeruginosa* PTCC 1570, were originally obtained from Pasteur Institute of Iran and Persian Type Culture Collection (PTCC), Tehran-Iran respectively.

The purity of each bacterium was confirmed by standard biochemical tests (30).

Preparation n-HA Ca-mineralized alginate beads

Cultures were grown in shaking incubators at 27 °C and 120 rpm for 24-48 h in capped 250 ml Erlenmeyer flasks containing nutrient broth medium (Merck, Germany).

Bacterial cell density was adjusted on 0.8-1 at 600 nm by UV-VIS scanning spectrophotometer, UV 2101 pc, Shimadzu (31).

Encapsulating bacteria in alginate beads

Alginate powder (Sigma–Aldrich Co.) 2% (w/v) was papered and autoclaved at 121 °C for 15 min. Bacterial inoculum was added to the alginate solution. The alginate/bacteria mixture (with stirring) was added drop by drop into a cold, sterile 0.2 M CaCl₂ solution through a sterile 1000 µL sampler. Gel beads of approximately 3 mm diameter were obtained. The beads were hardened by maintenance at downstairs fridge at 4 °C for 24 h. After that time, beads were transferred to BHI medium (50 ml) and were incubated at 32-35 °C. After approximately 48 h, the biofilm-coated alginate beads were transferred to mineral medium, which included calcium chloride (25 mM) and B-glycerophosphate disodium salt hydrate (50 mM) were used as calcium and phosphorus precursors, respectively at pH 8.6. After 14 days, alginate beads were dried at 60 °C for 5 h. Finally, dried beads were rubbed on each other to obtain the HA powder for analysis. The above-mentioned procedure was repeated for preparing control alginate beads to determine production ability of HA by two mentioned bacteria (32).

Preparation by transmitting alginate beads to medium contains 10% inoculation cultures of bacteria

For preparation n-HA by this procedure, alginate beads were prepared by pure alginate with 2% concentration then these beads were transferred to NB medium which contain 10% inoculation cultures of each bacterial strains, separately and the rest of test was repeated same major process (32).

Sol-gel as chemical method

The precursors used for preparation hydroxyapatite in this experiment were urea as ammonia donor and EDTA as the chelating agent to prevent immediate precipitate formation calcium in the course of gel formation ions, respectively.

Calcium nitrate tetrahydrate [Ca (NO₃)₂. 4H₂O] and ammonium dihydrogen phosphate [(NH₄) H₂PO₄] were used as calcium and phosphorus donors, respectively and ammonium solution as a basic solvent. (33).

Preparation of hydroxyapatite powder

EDTA (4.525 g/ml) ammonium solution (pH 9) was prepared and added to aqueous solution [calcium nitrate tetrahydrate (12.9 g), ammonium dihydrogen phosphate (3.9 g) and urea (4.25 g)] 2:1 (v/v). Solution was remained at 95 °C and continuously stirred for 2 h to produce milky white gel. According to calcinations procedure, gel was dried at 350 °C and 800 °C for 1 and 2 h, respectively (33).

Stereomicroscopy

Stereomicroscopic study was carried out by STMPRO-B, Italy instrument to distinguish bacterial growth and transfiguration of alginate beads at the end of test (34).

X-Ray Diffraction analysis

The crystal structure and the content phase present in prepared samples were analyzed with X-ray diffraction (XRD) by PANalitical, X'Pert PRO MRD (XL), Netherlands. The crystallite size of the powder was calculated from the XRD data by using the Scherrer equation as follow:

$$D = 0.9 k/b \cos h$$

Where:

D: the average crystallite size

k: the wavelength of X-rays (0.154 nm)

b: is the full width was measured at half-maximum of the HA, and

h; is the peak diffraction angle (7).

Fourier transform infra-red spectroscopy (FTIR)

The structure of obtained powders were determined by FTIR spectroscopy. These samples were analyzed by FTIR analysis (ASTM D3677, Germany) spectrometer in scanning range of 400-4000 cm⁻¹ (34).

Electron microscopy analysis

Scanning electron microscopy (EM3200, KYKY China) was used to characterize the morphology and determine the size of nanoparticle. Completely dried powder of hydroxyapatite obtained from chemical and microbial procedures, was mounted on aluminum specimen stub using an electrically conductive double-sided adhesive tape, and sputter-coated with gold alloy before examination in the microscope (34).

Thermogravimetric analysis

Thermogravimetric analysis (TGA) carried out by STA1500, Shinko Korea, in temperature region from 20 to 900 °C with heating rate 20 °C/min for HA produced by sol-gel method (35).

Results and Discussion

Stereomicroscopic analysis

The results showed that the surface of alginate beads encapsulated by two bacterial strains were covered with white precipitation of HA (Figure 1). In compared with the blank sample, it seems that metabolic and enzymatic activities of bacteria in the medium causes bioconversion of minerals precursor to HA and in this situation alginate works as an absorbent surface for precipitating this product. In this method the product is completely separated from medium and bacterial samples.

The existence of pure bacteria of each strain and their viability was confirmed by light microscopy through the direct examination of beads; and culturing of encapsulation bacteria separately in NA medium, Gram stain and observing under light microscope.

XRD analysis

The XRD patterns are shown in Figure 2 and 3, respectively.

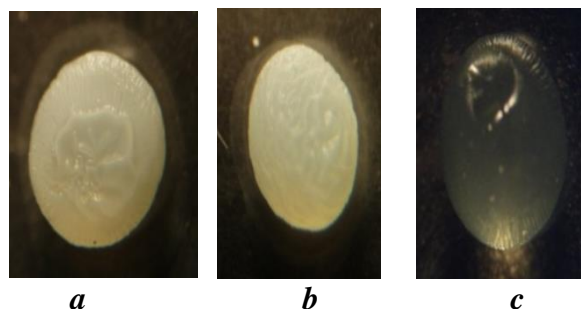


Figure 1. Alginate beads entrapped bacterial cells. **a)** Encapsulated form of *Ps. aeruginosa*, **b)** Control sample and **c)** Encapsulated form of *S. marcescens*.

In XRD patterns of obtained n-HA powders from sol-gel process and *S. marcescens*, there were some peaks indicating the presence of other phases such as calcium carbonate (CaCO_3) and small amounts of sodium chloride (approximately 1%) as impurity.

Although the presence of sodium ions within sample may not have adverse clinical effects because bone contains approximately 1% sodium (34) but the level of carbonate impurities in sol-gel methods can be controlled by regulating the aging time, solution and calcination temperatures (36).

However, the XRD pattern of n-HA produced by *P. aeruginosa* confirmed the purity of the prepared sample which is depicted in Figure 4.

The high intensity and broadening of the peaks show that the particles are highly crystalline in nano-scale size.

Second approach using *S. marcescens* had an ability to produce n-HA without impurity such as NaCl indicated by XRD. The average of crystallite size which was calculated by Scherrer equation was 4 nm. The XRD spectrum is shown in Figure 5. The average crystallite sizes of n-HA obtained using either sol-gel or encapsulation method by *S. marcescens* and *P. aeruginosa* estimated by Scherrer equation were 57, 5.8, 19.3 nm, respectively.

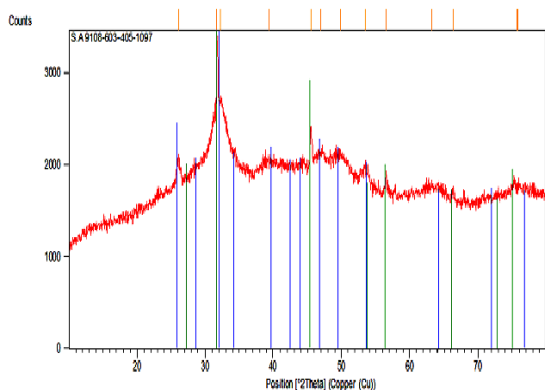


Figure 2. The XRD pattern of HA produced by *S. marcescens* encapsulated in alginate.

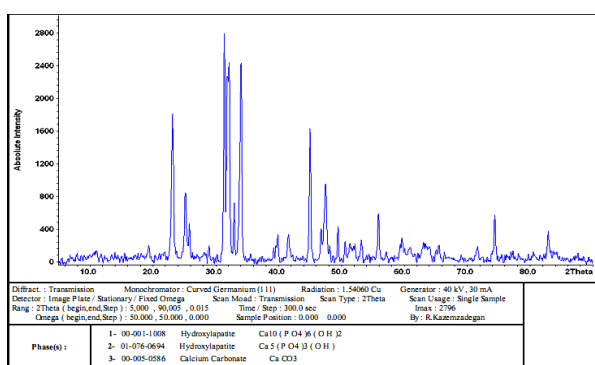


Figure 3. The XRD pattern of HA synthesized by sol-gel process.

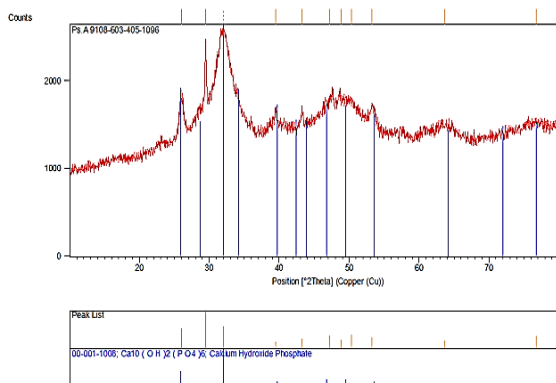


Figure 4. The XRD pattern of HA produced by *P. aeruginosa* encapsulated in alginate.

FTIR analysis

The FTIR spectroscopy has provided valuable information about the structure of HA powder. The FT-IR spectra of prepared samples from sol-gel process, *S. marcescens* and *P. aeruginosa* are shown in Figure 6, 7 and 8, respectively.

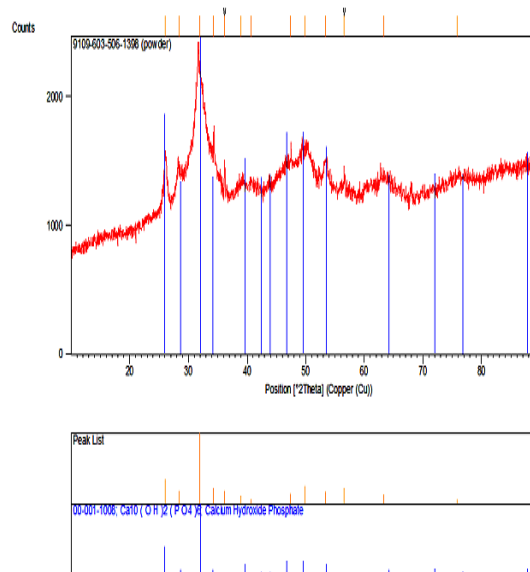


Figure 5. The XRD pattern of HA produced by inoculum of *S. marcescens* on alginate surface beads.

Presence of a weak peak in the region around 873 cm^{-1} indicates CO_3^{2-} band in sol-gel's sample confirming the minor amount of carbonate which was indicated in sol-gel XRD pattern.

The peak at $1104\text{-}1043\text{ cm}^{-1}$, $572\text{-}596\text{ cm}^{-1}$ and $470\text{-}471\text{ cm}^{-1}$ regions is indicative of P-O band in PO_4^{2-} and P-O-P band in PO_4^{3-} groups.

The peak at $860\text{-}877\text{ cm}^{-1}$ region indicates P-O-H band in HPO_4^- and the peak at $2600\text{-}3500\text{ cm}^{-1}$ regions is due to O-H bands. These peaks confirm the presence of HA phase in each sample (34).

The XRD patterns and FTIR spectra of synthesized HA were well consistent with reported values in the literature (9, 34, 37, 38).

SEM analysis

SEM micrographs of the n-HA powder from chemical and microbial procedures are shown in Figure 9, 10 and 11, respectively. The size of the particles were estimated around 37-67 nm for sol-gel sample. As compared to microbial samples, more agglomerate shapes were observed in chemical sample.

Nano-hydroxyapatite productivity by encapsulation method

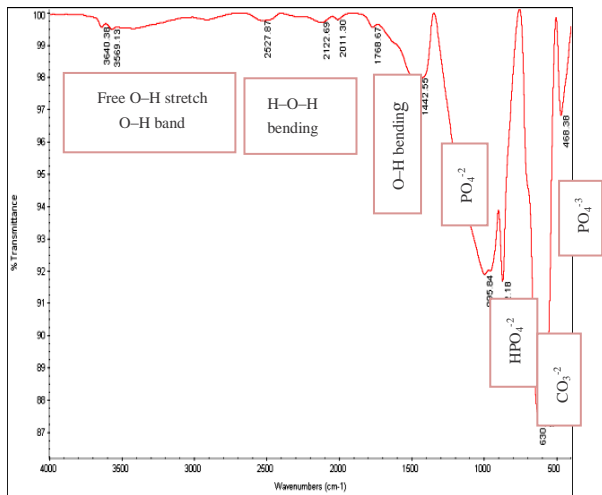


Figure 6. The FTIR spectrum of HA synthesized by sol-gel process.

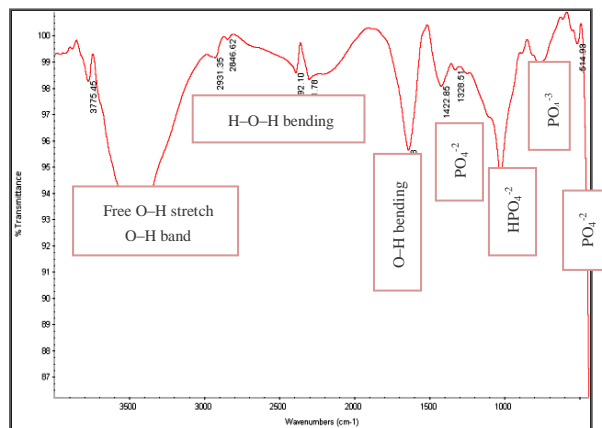


Figure 7. The FTIR spectrum of HA produced by *S. marcescens* encapsulated in alginate.

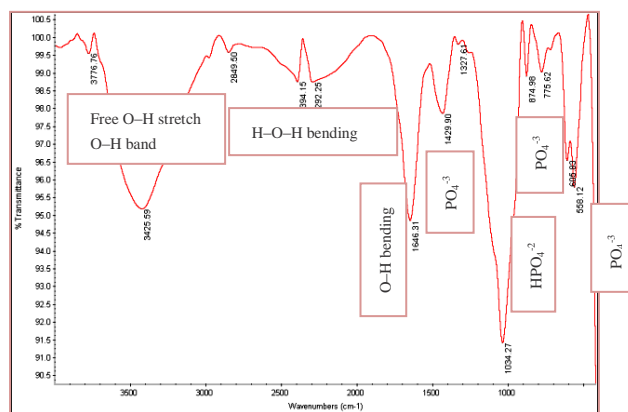


Figure 8. The FTIR spectrum of HA produced by *P. aeruginosa* encapsulated in alginate.

The presence of calcium carbonate crystal impurity was observed in HA synthesized by chemical method. The SEM images of HA were produced by *S. marcescences* and *P.*

aeruginosa have shown uniform and homogeneous distribution with circular shape in dimension around 8-55 nm and 15-37 nm, respectively.

Nanoparticle sizes and distribution of samples prepared by *S. marcescens* and *P. aeruginosa* showed comparable results with those reported previously (28, 29, 34) as well as with those prepared by chemical methods such as Sol-gel (11-27).

TGA Analysis

According to TG analysis, the HA sample was produced by sol-gel method showed little weight loss of around 1.169% up to 872 °C which is due to water evaporation demonstrating thermal stability of HA powder.

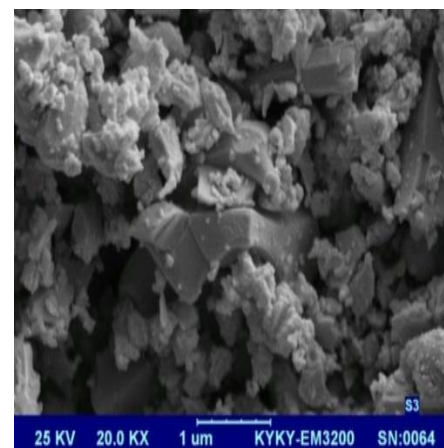
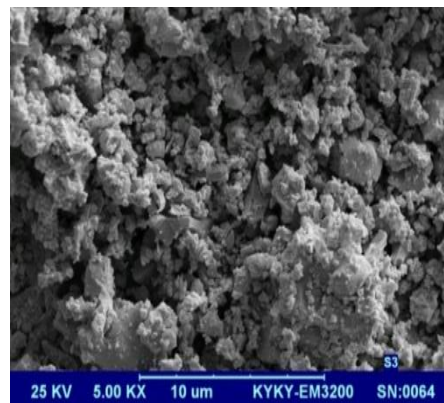


Figure 9. SEM images of HA synthesized by sol-gel method with 5.00 and 20.0 KX magnifications.

The presence of stoichiometric HAP with Ca/P ratio: 1.67). The TGA pattern is shown in (Figure 12).

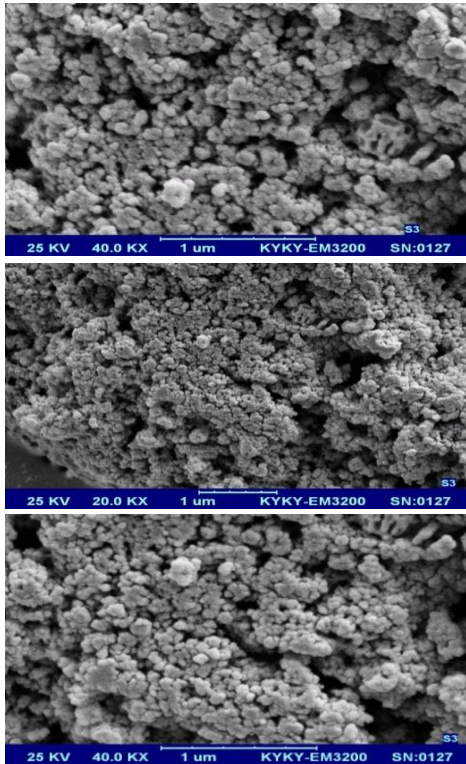


Figure 10. SEM images of HA produced by *S. marcescens* with 20 and 40 KX magnifications.

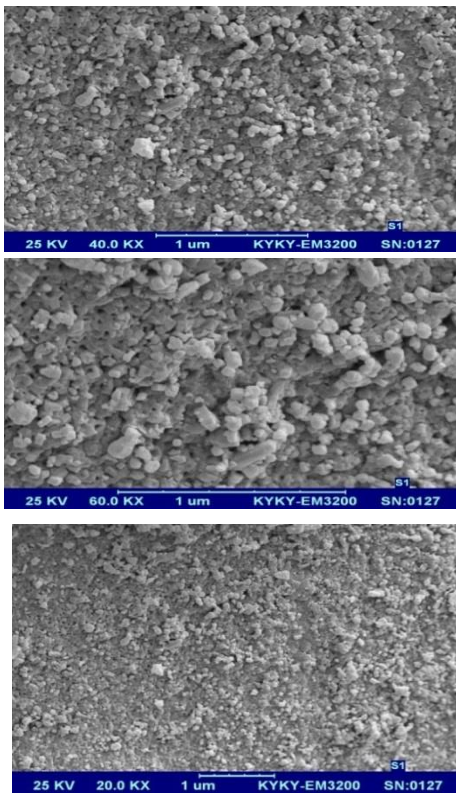


Figure 11. The SEM images of HA produced by *Ps. aeruginosa* with 20.0, 40.0 and 60.0 KX magnifications.

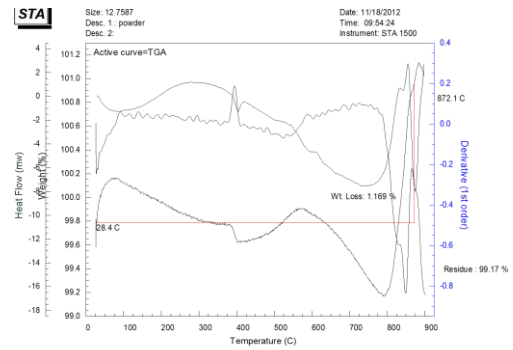


Figure 12. TGA pattern of the sol-gel sample.

Conclusions

According to the results, it seems chemical methods such as Sol-gel required more control over experimental variables. However, it is not economical because of expensive precursors.

The results of this study indicates that by using bacteria for the production of HA is cheap and the procedure is non-toxic resulting in HA similar to natural bone making it a suitable candidate for dental and medical applications.

Acknowledgments

The authors would like to thank Dr. Reza Marandi, University Vice-Chancellor, and assistance of microbiology laboratory for providing research facility.

References

1. Chai CS, Ben-Nissan B. Bioactive nanocrystalline sol-gel hydroxyapatite coatings. *J Mater Sci: Mater Med.* 1999; 10: 465-469.
2. Nayak AK. Hydroxyapatite Synthesis Methodologies: An Overview. *Int J Chem Tech Res.* 2010; 2(2): 903-907.
3. Ahmad Ramli R, Adnan R, Abu Bakar M, Malik Masudi S. Synthesis and Characterisation of Pure Nanoporous Hydroxyapatite. *J Phys Sci.* 2011; 2(1): 25-37.
4. Rajkumar M, Meenakshisundaram N, Rajendran V. Development of nanocomposites based on hydroxyapatite/sodium alginate: Synthesis and characterisation. *Mater Charact.* 2011; 62: 469-479.
5. Beganskiene A, Dudko O, Sirutkaitis R, Giraitis R. Water Based Sol-Gel Synthesis of Hydroxyapatite. *Mater Sci.* 2003; 9(4): 383-386.

Nano-hydroxyapatite productivity by encapsulation method

6. Sanosh KP, Min-Cheol C, Balakrishnan N, Kim TN, Seong-Jai C. Preparation and characterization of nano-hydroxyapatite powder using sol-gel technique. *Bull Mater Sci.* 2009; 32(5): 465-470.
7. Nikpour MR, Rabiee SM, Jahanshahi M. Synthesis and characterization of hydroxyapatite e/chitosan nanocomposite materials for medical engineering applications. *Compos Part B.* 2012; 43: 1881-1886.
8. Balamurugan A, Michel J, Faure J, Benhayoune H, Wortham L, Sockalingum G, Banchet V, Bouthors S, Laurent-Maquin D, Balossier G. Synthesis and structural analysis of sol-gel monophasic hydroxyapatite. *Ceram-Silik.* 2006; 50(1): 27-31.
9. Zadeegan S, Hossainipour M, Ghassai H, Rezaie HR, Naimi-Jamal MR. Synthesis of Cellulose-nanohydroxyapatite composite in 1-n-butyl-3-methylimidazolium chloride. *Ceram Int.* 2010; 36: 2375-2381.
10. Huang SB, Gao SS, Yu HY. Effect of nano-hydroxyapatite concentration on remineralization of initial enamel lesion in vitro. *Biomed Mater.* 2009; 4: 034104 (6pp).
11. Toriyama M, Ravaglioli A, Krajewski A, Gelotti G, Piancastelli A. Synthesis of hydroxyapatite-based powders by mechano-chemical method and their sintering. *J Eur Ceram Soc.* 1997; 16: 429-436.
12. Silva CC, Pinheiro AG, Miranda MAR., Góes JC, Sombra ASB. Structural properties of hydroxyapatite obtained by mechanosynthesis. *Solid State Sci.* 2003; 5(4): 553-558.
13. Otsuka M, Matsuda Y, Hsu J, Fox J, Higuchi W. Mechanochemical synthesis of bioactive material: Effect of environmental conditions on the phase transformation of calcium phosphates during grinding. *Bio-Med Mater Eng.* 1994; 4: 357-362.
14. Yoshimura M, Suda H, Okamoto K, Ioku K. Hydrothermal Synthesis of Biocompatible Whiskers. *J Mater Sci.* 1994; 29: 3339-3402.
15. Liu M, Chin T, Lai L, Chiu S, Chung K, Chang C. Hydroxyapatite Synthesized by Simplified Hydrothermal Method. *Ceram Int.* 1997; 23: 19-25.
16. Kimura I. Synthesis of hydroxyapatite by interfacial reaction in a multiple emulsion. *Res Lett Mater Sci.* 2007; 71284 (4pp).
17. Tas AC. Synthesis of biomimetic Ca-hydroxyapatite powders at 37 degrees in synthetic body fluids. *Biomaterials.* 2000; 21: 1429-1438.
18. Thamaraiselvi TV, Prabakaran K, Rajeswari S. Synthesis of hydroxyapatite that mimic bone mineralogy. *Trends Biomater Artif Org.* 2006; 19(2): 81-83.
19. Santos MH, de Oliveira M, de Freitas Souza P, Mansur HS, Vasconcelos WL. Synthesis control and characterization of hydroxyapatite prepared by wet precipitation process. *Mater Res.* 2004; 7(4): 625-630.
20. Manuel CM, Ferraz MP, Monteiro FJ. Synthesis of hydroxyapatite and tricalcium phosphate nanoparticles, Preliminary Studies. *Key Eng Mater.* 2003; 240-242: 555-58.
21. Shikhanzadeh M. Direct formation of nanophase hydroxyapatite on cathodically polarized electrodes. *J Mater Sci Mater Med.* 1998; 9(2): 67-72.
22. Suchanek W, Yoshimura M. Processing and properties of hydroxyapatite based biomaterials for use as hard tissue replacement implants. *J Mater Res.* 1998; 13: 94-117.
23. Elliott JC. *Structure and Chemistry of the Apatites and other Calcium Orthophosphates.* Elsevier Science, Amsterdam, The Netherlands; 1994.
24. Brendel T, Engel A, Russel C. Hydroxyapatite coating by polymeric route. *J Mater Sci Mater Med.* 1992; 3: 175-179.
25. Takahashi H, Yashima M, Kakihana M, Yoshimura M. Synthesis of stoichiometric hydroxyapatite by a gel route from the aqueous solution of citric and phosphonic acids. *Eur J Solid State Inorg Chem.* 1995; 32: 829-835.
26. Haddow DB, James PF, Van Noort R. Characterization of sol-gel surfaces for biomedical applications. *J Mater Sci Mater Med.* 1996; 7: 255-260.
27. Vijayalakshmi U, Rajeswari S. Preparation and characterization of micro crystalline hydroxyapatite using sol-gel method. *Trends Mater Artif Org.* 2006; 19(2): 57-62.
28. Macaskie LE, et al. A Novel Non Line-of-sight Method for Coating Hydroxyapatite onto the Surfaces of Support Materials by Biomineralization. *J Biotechnol.* 2005; 118: 187-200.
29. B, Fathi MH, Sheikh-Zeinoddin M, Soleimani-Zad S. Bacterial synthesis of nanostructured hydroxyapatite using *Serratia marcescens* PTCC 1187. *Int J Nanotechnol.* 2009; 6(10-11): 1015-1030.

30. Khanafari A, Hosseini F. *Practical Microbiology with Biochemical Function and Color Atlas*, Poorsina Pulplication, 1998.
31. Baron E, Finegold S. *Diagnostic Microbiology*, St Louis: CV Mosby Company; 8th edition, 1986; 89: 7-9.
32. Beshay U. Production of alkaline protease by *Teredinobacter turnirae* cells immobilized in Ca-alginate beads. *Afr J Biotech*. 2003; 2: 60-65.
33. Sopyan I, Sing R, Hamdi M. Synthesis of Nano Sized Hydroxyapatite Powder Using Sol-gel Technique and Its Conversion to Dense and Porous Bodies. *Indian J Chem*. 2008; 47: 1626-1631.
34. Sammons RL, Thackray AC, Mediledo H, Marquis PM, Jones IP, Yong P, Macaskie LE. Characterisation and sintering of nanohydroxyapatite synthesised by species of *Serratia*. *J Phys Conf Ser*. 2007; 93(1).
35. Zebarjad M, Feiz B, Shahtahmasebi N, Sajjadi A. Investigation on Stability of Nano-Hydroxyapatite Produced Using Precipitation Method at Sterile Condition. *MJME*. 2009; 3(2): 36-44.
36. Eshtiagh-Hosseini H, Housaindokht MR, Chahkandi M. Effects of parameters of sol-gel process on the phase evolution of sol-gel derived hydroxyapatite. *Mater Chem Phys*. 2007; 106(2): 310-316.
37. Ota Y, Iwashita T, Kasuga T. Novel preparation method of hydroxyapatite fibers. *J Am Ceram Soc*. 1998; 81: 1665-1668.
38. Kothapalli C, Wei M, Vasiliev A, Shaw M. Influence of temperature and concentration on the sintering behaviour and mechanical properties of hydroxyapatite. *J Acta Mater*. 2004; 52: 5655-5663.